

Magnetic Excitations of $\text{CsMn}(\text{SO}_4)_2 \cdot 12\text{D}_2\text{O}$, Measured by Inelastic Neutron Scattering

Reto Basler,[‡] Philip L. W. Tregenna-Piggott,^{*,‡}
Hanspeter Andres,[‡] Christopher Dobe,[‡] Hans-Ulrich Güdel,[‡]
Stefan Janssen,[†] and Garry J. McIntyre[§]

Department of Chemistry and Biochemistry
University of Bern, Freiestrasse 3, 3000 Bern 9, Switzerland
Laboratory for Neutron Scattering, PSI & ETHZ
CH-5232 Villigen PSI, Switzerland
Institute Laue Langevin, Avenue des Martyrs
BP156, F- 38042 Grenoble Cedex 9, France

Received October 30, 2000

The characterization of the ground state electronic structure of non-Kramers transition metal ions has always posed a serious experimental problem. This is because conventional EPR spectroscopy is usually confined to the detection of “forbidden” transitions, as the energies of the $\Delta m_s = \pm 1$ transitions can rarely be bridged using commercial spectrometers. In recent years, efforts to redress the dearth of experimental data have concentrated on utilizing the high-field, multi-frequency EPR technique.^{1–5} It is the purpose of this communication to show that under favorable circumstances, the energies of the low-energy excitations can be determined more directly, and more precisely, using the technique of inelastic neutron scattering (INS).

INS measurements were performed on powdered $\text{CsMn}(\text{SO}_4)_2 \cdot 12\text{D}_2\text{O}$, prepared from manganese(III) acetate, cesium sulfate, and D_2SO_4 (6 M),⁶ and recrystallized from D_2SO_4 (6 M). The compound was prepared close to fully deuterated, as the large incoherent neutron cross section of the proton often precludes the possibility of observing INS transitions. This compound undergoes a cubic (*Pa3*) to orthorhombic (*Pbca*) phase transition at ~ 156 K, driven by the cooperative Jahn–Teller effect, resulting in the lowering of the site symmetry of the $[\text{Mn}(\text{OD}_2)_6]^{3+}$ cation from S_6 to C_i .⁷ Consequently, the ${}^5\text{E}_g$ (S_6) ground term is split into ${}^5\text{A}_g \oplus {}^5\text{A}_g$ (C_i) components, the magnitude of which has been determined to be ~ 10500 cm^{-1} by absorption spectroscopy.⁸ Low temperature neutron diffraction measurements have shown that below the transition temperature, the aqua ion is tetragonally elongated, with Mn–O bond distances of 2.129(2), 1.929(1), and 1.924(1) Å (5 K), and all O–Mn–O bond angles within 1.4° of 90°. The ligand field also has a large trigonal component, which is manifested primarily by a concomitant rotation of the water molecules about the Mn–O bond vectors, to accommodate the hydrogen-bonding constraints of the lattice.^{7,9}

In Figure 1 are shown INS spectra of $\text{CsMn}(\text{SO}_4)_2 \cdot 12\text{D}_2\text{O}$ at temperatures of 1.5, 15, and 30 K, recorded on the time-of-flight spectrometer FOCUS at the Paul Scherrer Institute (PSI) in Villigen, Switzerland.¹⁰ An incident neutron wavelength of $\lambda = 5.32$ Å was selected, which afforded an energy-transfer window

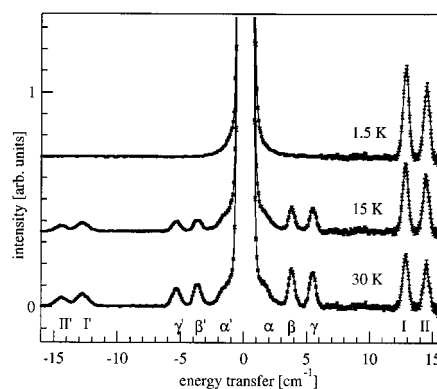


Figure 1. INS spectra of $\text{CsMn}(\text{SO}_4)_2 \cdot 12\text{D}_2\text{O}$ recorded at $T = 1.5$, 15 and 30 K measured on FOCUS with an incident neutron wavelength of $\lambda = 5.32$ Å. The transitions are labeled at the bottom of the figure.

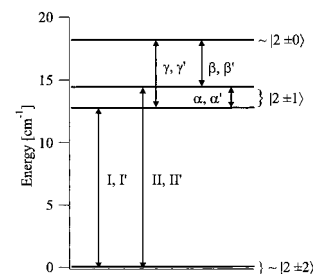


Figure 2. Experimentally determined energy-level diagram of the zero-field splitting in the ground state of $\text{CsMn}(\text{SO}_4)_2 \cdot 12\text{D}_2\text{O}$. The observed transitions are depicted as arrows and labeled as in Figure 1.

ranging from -16 cm^{-1} (neutron energy gain) to $+16$ cm^{-1} (neutron energy loss) with a resolution of 0.52 cm^{-1} . The spectrum at 1.5 K can be reproduced with a linear background and the superposition of two Gaussian functions, I and II, of equal width, centered at $12.795(6)$ cm^{-1} and $14.44(1)$ cm^{-1} , respectively, on the neutron energy-loss side. As the temperature is increased to 15 and 30 K, three hot transitions, α , β , γ , emerge with energies $1.61(2)$, $3.747(6)$, and $5.418(6)$ cm^{-1} , respectively. All transitions are also observed on the neutron energy-gain side (designated by primed labels) at elevated temperatures. On the basis of these results, the energy level diagram shown in Figure 2 could be derived. Arrows show the experimentally observed transitions within the five sublevels. The experimental energies and intensities are presented in Table 1.

The splitting of the ${}^5\text{A}_g$ (C_i) ground term can be described using the following effective spin Hamiltonian, acting in a basis of the five $S = 2$ spin functions,

$$\hat{H} = D \left[\hat{S}_z^2 - \frac{1}{3} S(S+1) \right] + E [\hat{S}_x^2 - \hat{S}_y^2] \quad (1)$$

where D and E are the axial and rhombic zero-field-splitting (ZFS) parameters, respectively. Least-squares refinement of the eigenvalues of eq 1 to the observed excitation energies yielded $D = -4.524(1)$ cm^{-1} and $E = 0.276(1)$ cm^{-1} , to give the calculated energy-levels and wave functions listed in Table 2. No significant improvement in the fit was obtained by including higher-order terms.

(10) Approximately 8 g of the compound was ground to a fine powder and sealed in an aluminium container. The detectors were calibrated by means of a vanadium metal spectrum; the time-of-flight to energy conversion and data reduction were performed with the standard program NINX at PSI. The data treatment involved the subtraction of a background spectrum of an empty aluminium container and subsequent analysis using the commercial program IGOR (WaveMetrics).

* To whom correspondence should be addressed.

[‡] University of Bern.

[†] Laboratory for Neutron Scattering, PSI & ETHZ.

[§] Institute Laue Langevin.

(1) Barra, A.-L.; Gatteschi, D.; Sessoli, R.; Abbati, G. L.; Cornia, A.; Fabretti, A. C.; Uytterhoeven, M. G. *Angew. Chem., Int. Ed. Engl.* **1997**, *36*, 2329.

(2) Telsler, J.; Pardi, L. A.; Krzystek, J.; Brunel, L.-C. *Inorg. Chem.* **1998**, *37*, 5769.

(3) Krzystek, J.; Telsler, J.; Pardi, L. A.; Goldberg, D. P.; Hoffman, B. M.; Brunel, L.-C. *Inorg. Chem.* **1999**, *38*, 6121.

(4) Tregenna-Piggott, P. L. W.; Weihe, H.; Bendix, J.; Barra, A.-L.; Güdel, H.-U. *Inorg. Chem.* **1999**, *38*, 5928.

(5) Knapp, M. J.; Krzystek, J.; Brunel, L.-C.; Hendrickson, N. *Inorg. Chem.* **2000**, *39*, 281.

(6) Christensen, O. T. *Z. Anorg. Chem.* **1901**, *27*, 329.

(7) Andres, H.-P.; Best, S. P.; Güdel, H.-U.; McIntyre, G.; Tregenna-Piggott, P. L. W. Manuscript in preparation.

(8) Johnson, D. A.; Nelson, P. G. *Inorg. Chem.* **1999**, *38*, 4949.

(9) Best, S. P.; Forsyth, J. B. *J. Chem. Soc., Dalton Trans.* **1991**, 1721.

Table 1. Experimental, and Theoretical, Energies and Relative Intensities of the INS Transitions^a

label	energy [cm ⁻¹]		normalized intensities					
	exp	calc	1.5 K		15 K		30 K	
			exp	calc	exp	calc	exp	calc
I	12.795 ± 0.006	12.794	1.00 ± 0.02	1.00	0.72 ± 0.03	0.73	0.56 ± 0.02	0.58
II	14.44 ± 0.01	14.45	0.81 ± 0.04	0.83	0.62 ± 0.04	0.61	0.46 ± 0.04	0.48
α	1.61 ± 0.02	1.66	—	—	0.156 ± 0.007	0.099	0.22 ± 0.01	0.14
β	3.747 ± 0.006	3.746	—	—	0.220 ± 0.009	0.267	0.39 ± 0.01	0.42
γ	5.418 ± 0.006	5.402	—	—	0.25 ± 0.01	0.28	0.38 ± 0.01	0.40
I'	-12.797 ± 0.007	12.794	—	—	0.179 ± 0.005	0.216	0.271 ± 0.005	0.312
II'	-14.46 ± 0.01	14.45	—	—	0.117 ± 0.005	0.154	0.190 ± 0.006	0.241
α'	-1.758 ± 0.008	1.656	—	—	0.045 ± 0.003	0.084	0.085 ± 0.004	0.132
β'	-3.715 ± 0.006	3.746	—	—	0.15 ± 0.01	0.19	0.28 ± 0.01	0.35
γ'	-5.400 ± 0.006	5.402	—	—	0.147 ± 0.005	0.165	0.267 ± 0.007	0.311

^a The experimental intensities were scaled against transition I at 1.5 K. The theoretical energies were calculated using eq 1 with the parameters $D = -4.524$ cm⁻¹ and $E = 0.276$ cm⁻¹. The intensities were calculated using eq 2, and the wave functions listed in Table 2.

Table 2. Calculated Energy Levels with Corresponding Wavefunctions Expanded in the Basis $|SM_s\rangle$ Obtained Using Eq 1

calculated energy [cm ⁻¹]	wave functions $ SM_s\rangle$
0	-0.7061 2 -2> - 0.0526 2 0> - 0.7061 2 +2>
0.050(4)	-0.7071 2 -2> + 0.7071 2 +2>
12.794(5)	-0.7071 2 -1> - 0.7071 2 +1>
14.450(5)	+0.7071 2 -1> - 0.7071 2 +1>
18.197(4)	+0.0372 2 -2> - 0.9986 2 0> + 0.0372 2 +2>

Neighboring manganese(III) cations in this compound are well-separated by two water molecules and a sulfate anion, and the INS data provide no indication of intermolecular magnetic interactions in the temperature and energy range of this study. The relative intensities of the INS transitions can be calculated using the wave functions given in table and employing the dipole approximation for N noninteracting ions; the differential neutron cross section is then given by,¹¹

$$\frac{d^2\sigma}{d\Omega d\omega} = N \left[\frac{\gamma e^2 g}{2mc^2} \right]^2 \cdot F^2(Q) \cdot \frac{|k_f|}{|k_i|} \sum_{if} \rho_i \cdot |\langle \psi_f | \hat{S}_\perp | \psi_i \rangle|^2 \cdot \delta \left(\frac{\Delta E}{\hbar} - \omega \right) \quad (2)$$

where $F(Q)$ is the magnetic form factor, k_i and k_f are the wavevectors of the incident and scattered neutrons, respectively, ρ_i is the Boltzman factor of a state i , $\gamma = -1.91$ is the gyromagnetic constant of the neutron, c is the speed of light, m and e are the mass and charge of the electron; \hat{S}_\perp is the component of the total spin operator perpendicular to the scattering vector Q . ψ_i and ψ_f denote the wave functions of the initial and final states. The cross section in eq 2 can be calculated at $Q = 0$ Å⁻¹, where $F(Q)$ is equal to unity. The problem is then reduced to the calculation of the squares of the transition moments:¹²

$$|\langle \psi_f | \hat{S}_\perp | \psi_i \rangle|^2 = \frac{1}{3} (2 |\langle \psi_f | \hat{S}_z | \psi_i \rangle|^2 + |\langle \psi_f | \hat{S}_+ | \psi_i \rangle|^2 + |\langle \psi_f | \hat{S}_- | \psi_i \rangle|^2) \quad (3)$$

The calculated energies and relative intensities for all temperatures are presented alongside the experimental values in Table 1, where the agreement is seen to be excellent for the energies and very good for the intensities.

The zero-field-splitting parameters for the $[\text{Mn}(\text{OD}_2)_6]^{3+}$ are very similar to those determined for the $\text{Mn}(\text{dmb})_3$ complex ($D = -4.35$, $E = 0.26$ cm⁻¹),¹ where Hdmb is 1,3-diphenyl-1,3-propanedione. Both complexes are homoleptic consisting of oxygen-donor ligands; in both cases the low-symmetry ligand field

is dominated by a strong tetragonal elongation, driven by the Jahn–Teller effect, giving rise to a splitting of the ${}^5E_g(O_h)$ ground term of comparable magnitudes.^{1,8} The dbm ligand is, however, expected to be more nephelauxetic compared to water, because of its conjugated chelate framework. The dominant contribution to the magnitude of D is expected to arise from spin–orbit coupling matrix elements between the ground ${}^5B_{1g}(D_{4h})$ and excited ${}^3E_g(D_{4h})$ terms.^{1,3} Although the optical transitions between these terms have not been reported for either system, a reduction in the nephelauxetic parameter β , would imply that the excited ${}^3E_g(D_{4h})$ term occurs at lower energy for the $\text{Mn}(\text{dbm})_3$ complex. The fact that the magnitude of D is similar for the $[\text{Mn}(\text{OD}_2)_6]^{3+}$ and $\text{Mn}(\text{dbm})_3$ complexes suggests that the likely reduction in the Racah parameters, upon replacing water with dbm, is matched by a reduction in the spin–orbit coupling constant, such that the ratio $\lambda^2/\Delta E({}^3E_g - {}^5B_{1g})$ is of similar order for both complexes. A measure of the degree of rhombicity is given by the ratio $|E/D|$, which is ~ 0.06 for both $[\text{Mn}(\text{OD}_2)_6]^{3+}$ and $\text{Mn}(\text{dbm})_3$. The structure of $\text{Mn}(\text{dbm})_3$ reveals the complex to be orthorhombic, and the values of D and E could be reproduced using the angular overlap model (AOM), considering the MnO_6 framework only.¹ Using the same approach, we have not been able to account for the degree of rhombicity found for $[\text{Mn}(\text{OD}_2)_6]^{3+}$, as the symmetry of the MnO_6 framework within the $[\text{Mn}(\text{OD}_2)_6]^{3+}$ cation is close to idealized D_{4h} . To reproduce the experimental data, the structure and bonding of the whole $[\text{Mn}(\text{OD}_2)_6]^{3+}$ complex needs to be considered. Our calculations suggest that a significant contribution to the magnitude of E arises as a consequence of the π -anisotropic nature of metal–water bonding;¹³ the calculated spin–Hamiltonian parameters are then dependent on the disposition of the deuterium atoms as they define the coordination geometry of the water molecules.¹⁴ The results of these calculations shall be presented in a future publication, along with high-field multi-frequency EPR data, which we have recently obtained.

In summary: the first INS study of a monomeric Mn(III) complex has been reported. It has been shown that these measurements afford the direct observation of the low-energy electronic excitations, from which the axial and orthorhombic zero-field spin–Hamiltonian parameters have been precisely determined. It may be concluded that the INS technique will be of great value in characterizing the electronic structure of other integer-spin transition metal ion complexes, provided the incoherent background of any H atoms can be avoided by complete deuteration.

Acknowledgment. We thank Høgni Weihe and Jesper Bendix for useful discussions. This work was funded by the Swiss National Science Foundation.

JA003801A

(11) Marshall, W.; Lovesey, S. W. *Theory of Thermal Neutron Scattering*; Oxford University Press: 1971.

(12) Birgenau, R. J. *J. Phys. Chem. Solids*. **1972**, *33*, 59.

(13) Best, S. P.; Figgis, B. N.; Forsyth, J. B.; Reynolds, P. A.; Tregenna-Piggott, P. L. W. *Inorg. Chem.* **1995**, *34*, 4605.

(14) Best, S. P.; Forsyth, J. B.; Tregenna-Piggott, P. L. W. *J. Chem. Soc., Dalton Trans.* **1993**, 2711.